Functional Hydrogel Surfaces: Binding Kinesin-Based Molecular Motor Proteins to Selected Patterned Sites

ARTICLE *in* ADVANCED FUNCTIONAL MATERIALS · AUGUST 2005

Impact Factor: 11.81 · DOI: 10.1002/adfm.200400117

5 AUTHORS, INCLUDING:

Qingkui Wang
Chinese Academy of Sciences
464 PUBLICATIONS **10,216** CITATIONS
SEE PROFILE

Christopher K Ober
Cornell University
587 PUBLICATIONS **15,869** CITATIONS
SEE PROFILE

Functional Hydrogel Surfaces: Binding Kinesin-Based Molecular Motor Proteins to Selected Patterned Sites**

By *Tianyue Yu*, *Qing Wang*, *Daniel S. Johnson*, *Michelle D. Wang*, and *Christopher K. Ober**

Hydrogel microstructures with micrometer-scale topography and controllable functionality have great potential for numerous nanobiotechnology applications including, for example, three-dimensional structures that exhibit controlled interactions with proteins and cells. Taking advantage of the strong affinity of histidine (His) residues for metal-ion–nitrilotriacetic acid (NTA) complexes, we have chemically modified hydrogels to enable protein immobilization with retention of activity by incorporating 2-methacrylamidobutyl nitrilotriacetic acid, an NTA-containing monomer that can be copolymerized with a series of monomers to form NTA-containing hydrogels. By varying the NTA-monomer composition in the hydrogels, it is possible to control the amount of protein bound to the hydrogel surface. The retention of biological activity was demonstrated by microtubule gliding assays. Normally, hydrogels are resistant to protein binding, but we have selected these materials because of their porous nature. Bringing together hydrogel functionalization and soft-lithography patterning techniques, it was possible to create a hybrid hydrogel superstructure that possesses binding specificity to His-tagged protein in selected sites. This type of surface and microstructure is not only advantageous for motor protein integration, but it can also be generally applied to the formation of His-tagged molecules for sensors and biochip applications.

1. Introduction

Biological molecular motor proteins are molecules in cells that are responsible for producing cellular movements, such as muscle contraction, vesicle transport, cell division, and gene expression.[1–4] Linear molecular motors convert chemical energy into mechanical movement by unidirectional translocation on long biological polymers, such as kinesin, which may be thought of as "tracks" for molecular motor proteins. The kinesin–microtubule system is an example of such a biological molecular motor pair, where kinesin is the molecular motor and the microtubule is the track.[5] From load–velocity experiments, it has been shown that a single kinesin molecule is capable of generating a ≈ 5 pN stall force by taking 8 nm steps with an energy-conversion efficiency of ≈ 50 %.[2,3] With the development of molecular biology, the microtubule tracks can be reassembled in vitro from purified tubulin, and kinesin motors can be produced using recombinant methods in bacteria. Recombinant kinesin can also be genetically engineered to have specific interactions with other molecules.[6] Taking into consideration the motor protein's nanometer dimensions, its power-converting efficiency, and the readily available techniques for manipulating these proteins, it should be possible to develop useful nanomachines powered by these motor proteins. For example, one can imagine a type of nanomachine in which kinesin molecules transport "cargo" along microtubule tracks, or another type of nanomachine where a wheel/well combination converts the linear motion of the kinesin/microtubule combination to the rotational motion of a wheel (Fig. 1).

The ability to harness the motion of microtubules is a key step toward molecular motor devices. Two different approaches to engineering kinesin-coated guide pathways for microtubules have been attempted. One approach to forming such "paths" was achieved by spatially defining the binding of the

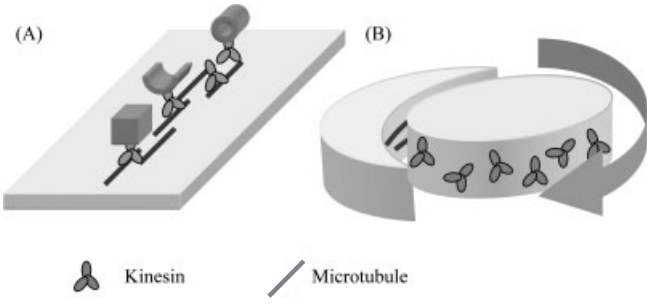

Figure 1. A) A nanomachine that transports particles. B) Nanomachines with a wheel.

[*] Prof. C. K. Ober, Dr. T. Yu[+]
Materials Science and Engineering, Cornell University
Ithaca, NY 14853 (USA)
E-mail: cober@ccmr.cornell.edu
Prof. Q. Wang
Materials Science and Engineering, Penn State University
University Park, PA 16802 (USA)
Dr. D. S. Johnson, Prof. M. D. Wang
Department of Physics, Cornell University
Ithaca, NY 14853 (USA)
[+] Present address: Affymetrix Inc., 3380 Central Expressway, Santa Clara, CA 95051, USA.

[**] This work was supported by the STC Program of the National Science Foundation under Agreement No. ECS-9876771 through the Nanobiotechnology Center in Cornell University. The use of the facilities of the Cornell Nanofabrication Facility and the Cornell Center for Materials Research is gratefully acknowledged. The authors thank Joe Howard at the Max Planck Institute of Molecular Cell Biology and Genetics for providing the plasmid for the kinesin used in this study.

 DOI: 10.1002/adfm.200400117

motor proteins to surfaces with patterned hydrophobic and hydrophilic regions.[7,8] Another approach focused on creating surface topography—either through nanogrooves made by shear-depositing poly(tetrafluoroethylene) (PTFE) films, or by using micrometer-scale channels and walls by replica molding—as a means to direct the motion of the microtubules on kinesin-coated surfaces.[9,10] Both methods have their shortcomings. The guiding mechanism of a microtubule's movement on a kinesin-coated surface is based on Brownian motion. The advancing end of the microtubule spatially fluctuates from side to side until it interacts with another kinesin molecule along its gliding direction.[10] In the former approach, the advancing microtubules may become trapped at the edge of the path, or even "derailed", owing to the discrete pattern of the motor-protein paths, so that the number of microtubules on the path gradually decreases over time.[11] In the latter approach, owing to the homogeneous coverage of motor proteins on the surface, a microtubule can escape any topographical confinement when it first binds to a sidewall, slowly climbs over, and then jumps to the next groove.[10] An optimal solution therefore is to achieve confined movement of microtubules by a combination of chemical specificity and topographical patterning.

Using hydrogel materials as the substrate for motor devices may provide several advantages. Hydrogels are crosslinked polymers that swell but do not dissolve in water. They are generally accepted as biocompatible materials, are widely used in the contact lens industry and biomedical devices, and hold great promise for tissue engineering and drug-delivery applications.[12,13] Their biocompatibility and ability to respond to their environment make them useful as interfacial materials and as an integral part in sensor applications. Because motor proteins function in an aqueous environment, hydrogels permit diffusion of adenosine triphosphate (ATP), the energy molecule, to a biological motor, thereby making them superior to many other materials. Hydrogels behave like an elastomer, but their dimensions can be controlled by their degree of swelling, which is controlled either by the chemical potential of the aqueous phase or by the crosslinking of the hydrogel. Hydrogels are also chemically versatile. Their composition and properties can be easily modified by many readily available chemistries and techniques.[14–16]

Specific protein binding to hydrogel materials has been demonstrated by incorporating metal chelators that serve to link the protein to the polymer.[17,18] Small affinity tags, widely used in protein handling, have simplified and improved the expression, purification, detection, and assay of recombinant proteins. The interaction between proteins tagged with six consecutive histidine (His) residues (6×His tag) and nickel–nitrilotriacetic acid (Ni-NTA) provides remarkable selectivity and strong affinity (Fig. 2).[19] NTA occupies four of the six ligand binding sites in the coordination sphere of the nickel ion; the two other sites are free to interact with the 6×His Tag to provide strong binding at the terminal amine and the nitrogen of the imidazole ring.[20] We synthesized 2-methacrylamidobutyl nitrilotriacetic acid, an NTA-containing monomer that can be copolymerized with a series of monomers to form NTA-containing hydrogels. After nickel-solution treatment, the hydrogels exhibit very strong binding to His-tagged proteins through Ni-NTA chelation. By varying the NTA monomer composition in the hydrogels, it is possible to control the amount of protein bound to the hydrogels. The retention of a protein's biological activity has been demonstrated by microtubule gliding assays.

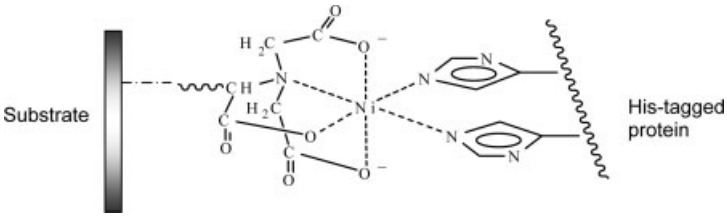

Figure 2. Scheme showing a His-tagged protein attached to a Ni-NTA-containing substrate.

Although this hydrated material is usually considered unsuitable for conventional patterning techniques, we have overcome many compatibility issues and developed processes to microfabricate hydrogels by combining photolithography and soft lithography.[21,22] Bringing together hydrogel functionalization and lithographic-patterning techniques, we have been able to create a hybrid hydrogel superstructure that possesses binding specificity in topographically patterned His-tagged regions. This kind of surface and microstructure is not only advantageous for motor device integration, but it can also be generally applied to the surface binding of His-tagged proteins to hydrogels for sensors and biochip applications.

2. Results and Discussion

2.1. Hydrogel Functionalization

Taking advantage of the strong affinity of His residues for a metal ion–NTA complex, we have chemically modified hydrogels for protein immobilization. 2-Hydroxyethyl methacrylate (HEMA) hydrogels are generally considered to be biocompatible and are widely used in the contact lens industry. HEMA hydrogels also have good mechanical properties suitable for use as a motor-device substrate. Unlike polyethylene glycol (PEG)-based hydrogels, where chemical modification can only be carried out by functionalizing chain ends, HEMA-based hydrogels permit the incorporation of various functional comonomers, and the pendent hydroxyl groups on the polymer backbone can serve as targeted functionalization sites. Therefore, we selected HEMA hydrogels as the model material for this study. A polymerizable acrylamide monomer with an NTA moiety was synthesized. The HEMA and NTA-containing HEMA hydrogels were synthesized by free-radical photopolymerization using 365 nm UV exposure. 2,2′-Dimethoxy-2-phenylacetophenone (DMPAP) was used as the photoinitiator; ethylene glycol dimethacrylate (EGDMA), in various concentrations, was used as the crosslinking agent. After treatment with $NiSO_4$, the NTA moiety could serve as a complexation

ADVANCED FUNCTIONAL MATERIALS

site to bind His-tagged proteins in an aqueous environment. The NTA-containing monomer can be readily copolymerized with other monomers, with its composition easily adjusted to control the amount of protein bound to the hydrogel surface (Fig. 3).

2.2. His-Tagged Protein Binding to NTA Hydrogels

A series of control studies were carried out to confirm the effectiveness of hydrogel functionalization for specific protein binding. A 6×His tag is relatively small, thus it does not interfere with the structure or function of the modified protein.[19] Fluorescently labeled *N*-terminal His-tagged ubiquitin (0.8 mg mL^{-1}) was used as a model protein to conduct protein-binding studies on the hydrogel surface. The fluorescent intensity from confocal microscopy studies may be directly related to the quantity of protein bound to the hydrogel. After nickel sulfate solution treatment, NTA-containing hydrogels exhibited a much stronger signal (and therefore higher protein concentration), due to the immobilization of His-tagged protein, than non-functionalized hydrogels at all tested protein concentrations (Fig. 4).

This important difference was caused by the incorporation of only 1 mol-% NTA in the substrate and thereby demonstrated the high sensitivity of the Ni-NTA–histidine interaction. Unmodified HEMA hydrogels showed minimal protein binding at most protein concentrations and gave a detectable signal only when incubated at the highest protein concentration (1:2 dilution). This undesirable absorption was due to non-specific binding and could be alleviated by increasing the number of wash cycles.

The capture of 6×His-tagged proteins by their affinity to metal chelates relies on two interactions: nickel–chelator and nickel–6×His. Both interactions are important for effective binding. The small dissociation constants of Ni-NTA and the

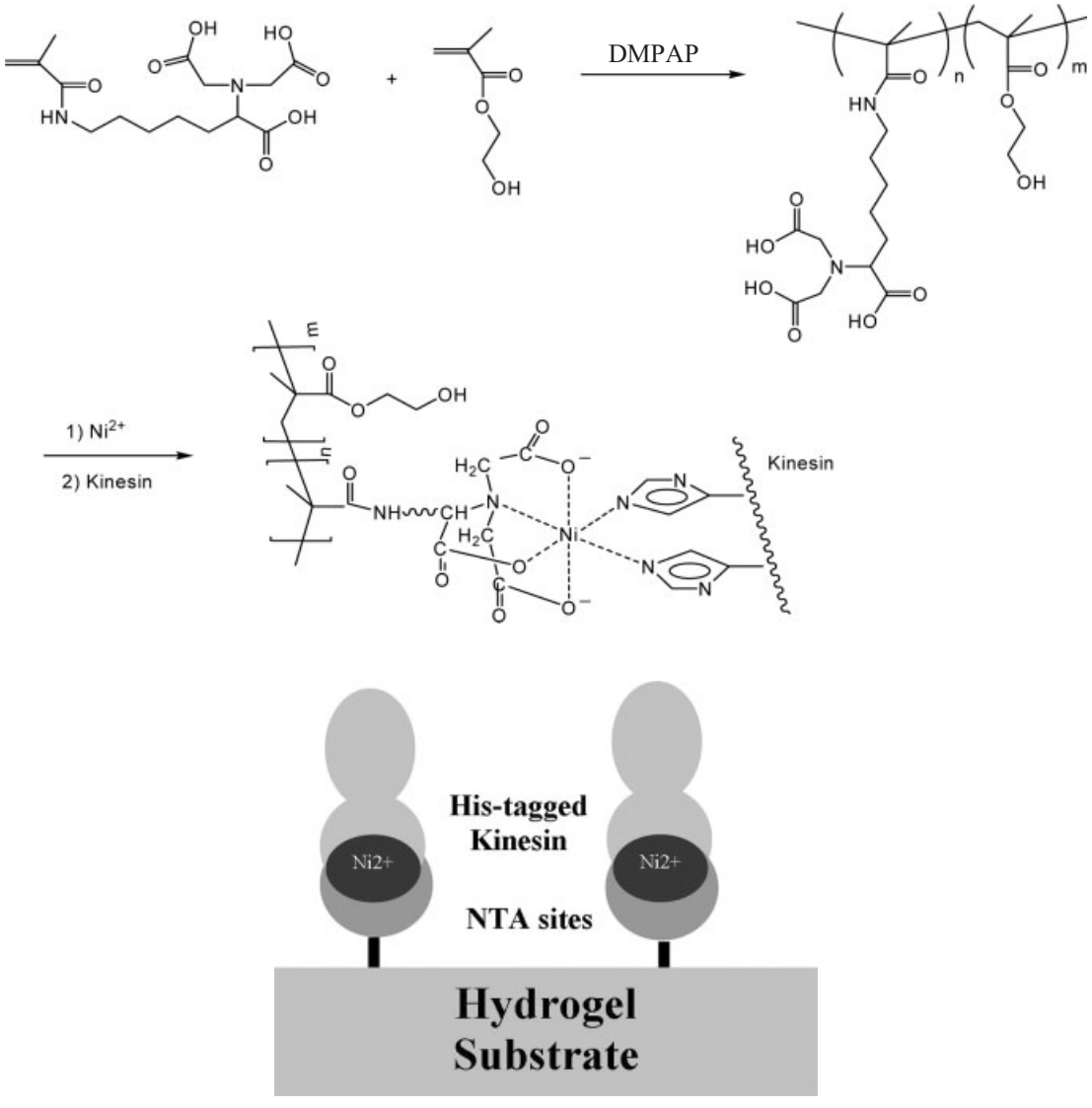

Figure 3. NTA-containing hydrogel synthesis and His-tagged protein binding through the Ni-NTA complex.

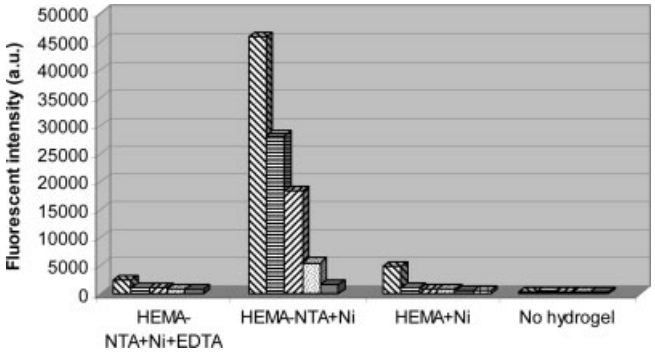

Figure 4. Comparison of protein binding for different hydrogel systems (dilutions were made from 0.8 mg mL^{-1} fluorescently labeled ubiquitin solution).

Ni-His tag, 10^{-15} and 10^{-13}, respectively, ensure the stable attachment of His-tagged proteins to the Ni-NTA sites.[23] Stronger chelators, such as ethylenediaminetetraacetic acid (EDTA), destroy the interaction of His-tagged protein with the Ni-NTA complex by competing effectively for the nickel ions on the NTA sites. As shown in Figure 4, when EDTA was included in the buffer, protein immobilization was suppressed to a level comparable to that of non-functionalized hydrogels. Even non-specific binding at the highest protein concentration was not as prominent because protein was lost as protein–Ni–EDTA complexes during the washing steps.

To control the amount of protein attached to the substrate, hydrogels with different NTA compositions were synthesized. After $NiSO_4$ treatment and protein incubation, fluorescent images of the hydrogel surface and vertical cross-section were acquired using confocal microscopy (Fig. 5). The fluorescence signal from the surface immobilized proteins formed a thin, bright horizontal streak in the cross-section image. Above this bright region is the aqueous solution and below it is the hydrogel with virtually no bound protein. An arbitrary line perpendicular to this streak was drawn on the image to obtain the signal intensity profile. Figure 6 shows the fluorescent intensity profiles of samples with different levels of NTA incorporation. The higher the NTA concentration in the sample, the stronger the fluorescence signal. Given a fixed NTA concentration in

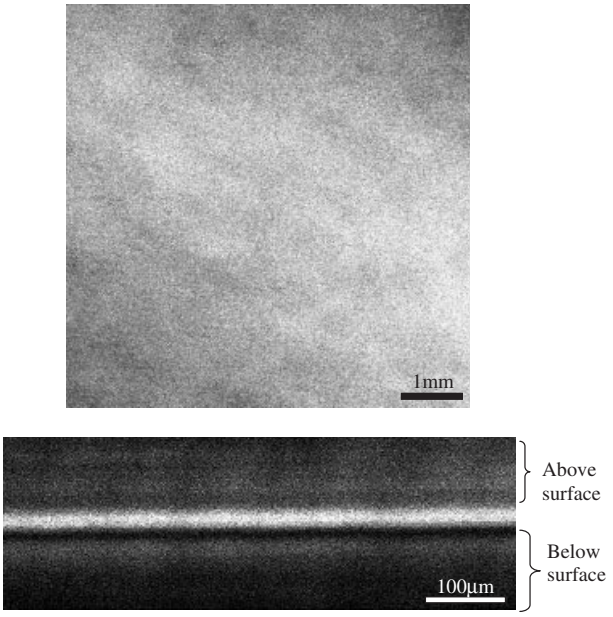

Figure 5. Confocal microscopy images of 1 mol-% NTA-containing hydrogel surface (top) and vertical cross-section view (bottom) after protein binding.

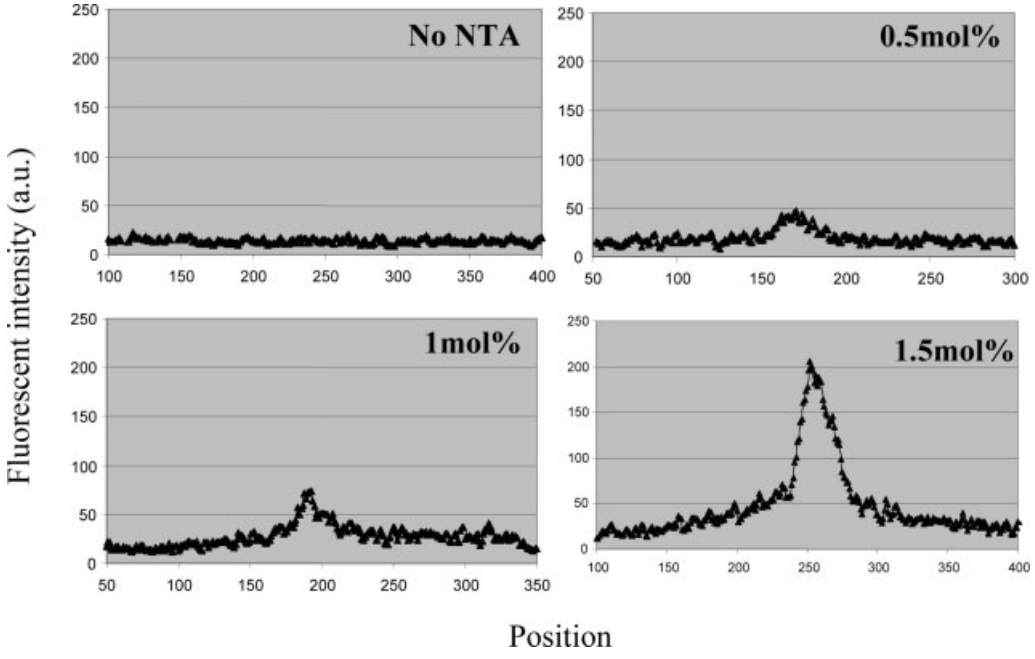

Figure 6. Vertical cross-section of fluorescent images for hydrogels with different NTA incorporation after protein binding.

ADVANCED FUNCTIONAL MATERIALS

the hydrogel, protein binding would be expected to saturate when the protein concentration exceeds the NTA-containing hydrogel's binding capacity. Figure 7 shows that the fluorescence signal intensity increases dramatically with protein concentration, reaching a plateau at around 0.17 mg mL^{-1}, for a 1 mol-% NTA-containing hydrogel.

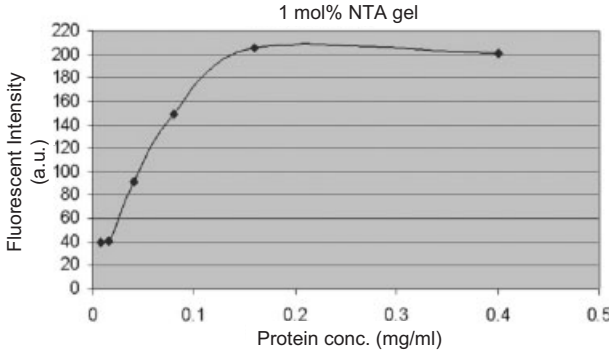

Figure 7. Fluorescent intensity indicating that protein binding to NTA-containing hydrogel increases as the protein concentration increases and reaches saturation at around 0.17 mg mL^{-1}.

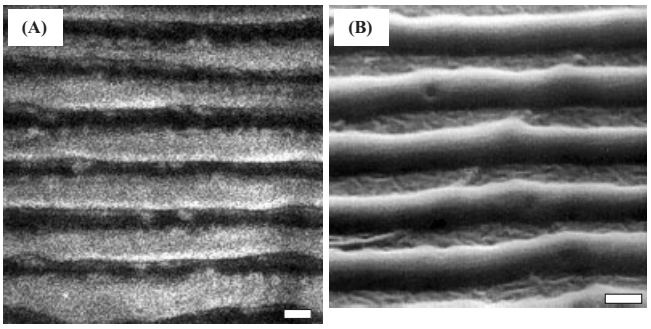

Figure 8. A) Fluorescent image of selective protein binding. B) SEM micrograph of patterned hydrogel microstructure (scale bars = 5 μm).

2.3. Protein Binding on a Hydrogel Surface in Predetermined Regions

Soft lithography was used to create hybrid hydrogel microstructures that exhibit specificity to His-tagged proteins in specified regions of the surface, while retaining the inert character in the other regions. The details of hydrogel patterning and hybrid hydrogel microfabrication have been described elsewhere.[21] Basically, an NTA-containing hydrogel was first synthesized between two glass slides. One slide was subsequently removed to yield a thin layer of NTA-containing hydrogel with a planar surface. A polydimethylsiloxane (PDMS) mold with the desired topographic pattern was cut to leave the channel ends open when placed on the hydrogel surface; conformal contact was formed between these two elastomeric surfaces. UV or thermally curable pre-gel solution was placed at the open ends of the channels and spontaneously filled the channels by capillarity. In this study, the PDMS mold contained channel patterns 5 μm wide and 1.5 μm deep, and a hydroxyethyl methacrylate pre-gel solution with photocrosslinker was used to fill the channels. After UV curing, the PDMS mold was removed and the patterned HEMA hydrogel was left on the NTA-containing hydrogel surface.

The resulting hybrid hydrogel microstructure has unique protein-binding characteristics. The unblocked NTA-modified hydrogel surfaces form the bottom of the trenches that provide regions for specific protein attachment; the inert HEMA hydrogel forms the walls that prevent unwanted protein binding. After nickel sulfate treatment, fluorescently labeled His-tagged ubiquitin was observed to bind only to the hydrogel surface in the predetermined regions. Figure 8 shows a fluorescence micrograph demonstrating such selective protein binding and a scanning electron microscopy (SEM) image revealing the topographic pattern on the hydrogel surface. By incorporating an asymmetric design into the topographic patterns, it is possible to realize the unidirectional gliding of microtubules on a kinesin-coated hydrogel surface.[24] Further study of the optimal surface density for microtubule attachment is underway to provide a better understanding of long-duration, unidirectional microtubule gliding.

2.4. Kinesin Activity After Binding to the Hydrogel Surface

Most prior studies involving motor-protein immobilization have been based on direct, non-specific adsorption of protein to the substrate, or on protein binding to surfactant molecules that are adsorbed on the substrate.[7–11] These attachment mechanisms are too fragile and unstable for our purposes. However, the overly tight binding of motor proteins to a substrate may hinder favorable interactions with other molecules, and therefore decrease biological activity. NTA-containing hydrogels should therefore be ideally suited to use as a substrate material because of their high conformational freedom and highly stable protein binding.

The retention of biological activity was demonstrated by microtubule gliding assays on the hydrogel surface. Open-ended flow chambers were assembled between a microscope slide and a coverslip separated by two strips of double-sided adhesive tape. A thin layer of NTA-containing hydrogel was polymerized and covalently bound to the surface-treated microscope slide. The flow chamber was placed on the microscope stage in such a way that the coverslip served as the bottom of the chamber and the glass slide coated with hydrogel served as the top of the chamber. The use of thin and transparent hydrogel layers made in-situ imaging of the microtubules convenient. Rhodamine-labeled microtubules were used for direct observation, and an oxygen scavenger system was added to reduce fluorescence bleaching. Sequences of images were captured by a charge-coupled device (CCD) camera and were analyzed with PC-based imaging software, SimplePCI. Figure 9 shows photographs representing snapshots of Rhodamine-labeled microtubules taken at intervals of 5.5 s. The motion of the micro-

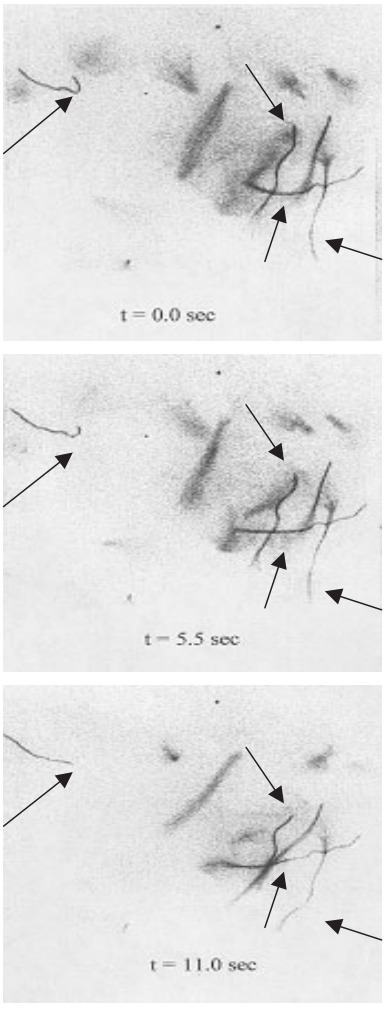

Figure 9. Microtubule movement on an NTA-containing hydrogel surface (full frame = 50 μm wide).

tubules was calculated to be 0.3 to 0.5 $\mu m\,s^{-1}$. This compares well to previously published data on microtubule motion—$\approx 0.8\ \mu m\,s^{-1}$[25]—and demonstrates that surface-bound kinesin motor proteins remain biologically active using this method of binding to HEMA-based hydrogels.

3. Conclusions

We have described the creation of functional hydrogel surfaces for molecular-motor devices. A polymerizable acrylamide monomer with an NTA moiety was synthesized and incorporated into HEMA hydrogels in a controlled fashion. This approach was shown to be an effective means for specific protein immobilization. Protein immobilization on the NTA-containing hydrogel surface was characterized by various methods and selective protein binding on hybrid hydrogel microstructures was demonstrated. The retention of biological activity of the kinesin motor protein after attachment to the functionalized hydrogel surface was demonstrated by a microtubule gliding assay. Such functional hydrogel surfaces may be very useful for microtubule motility studies, as well as for biosensor and biochip applications.

4. Experimental

Materials: HEMA, the crosslinking agent EGDMA, and the photoinitiator DMPAP were obtained from Aldrich (Milwaukee, WI) and used without further purification. The surface adhesion promoters methacryloxypropyl trimethoxysilane and trichloro(1*H*,1*H*,2*H*,2*H*-perfluorooctyl)silane were purchased from Gelest. Poly(dimethylsiloxane) (Sylgard 184) was obtained from Dow Corning. The model protein *N*-terminal 6×His-tagged ubiquitin was purchased from Sigma-Aldrich. The Alexa Fluor 488 protein-labeling kit was obtained from Molecular Probes and used as instructed.

Instrumentation: Photocrosslinking and hydrogel patterning were carried out using an HTG System 3HR Contact/Proximity Aligner tool. The ultraviolet exposure wavelength was 365 nm with an average intensity of around 30 $mW\,cm^{-2}$. The film thickness was measured using a Tencor AlphaStep 200 Surface Profilometer. Scanning electron microscopy was carried out on a Zeiss 982 SEM at the Cornell Nanofabrication Facility (CNF). Atomic force microscopy (AFM) was carried out using a Digital Instrument Dimension 3100 AFM at CNF. The fluorescence images were collected by an Olympus IX-70 inverted microscope coupled to a BioRad MRC 1024 confocal scan box with three channels for image acquisition. The confocal microscope was excited by an air-cooled krypton–argon laser (488 nm, 568 nm, and 647 nm). Movement of fluorescent microtubules was observed with a 100×, 1.3 numerical aperture, oil-immersion objective on an Eclipse TE200 inverted microscope (Nikon USA, Melville, NY) with an epifluorescence attachment (Nikon USA, Melville, NY). The hydrogel specimen plane was illuminated and observed from below. Images were captured via a C4742-95-12ER cooled CCD camera (Hamamatsu, Bridgewater, NJ). Sequences of images were captured and analyzed with the PC-based imaging software, SimplePCI (Compix Inc., Cranberry, PA).

Synthesis of NTA-Containing HEMA Hydrogel: The monomer with a nitrilotriacetic acid moiety, *Nε*-(2-methyl-1-oxopropenyl)-*Nα*-bis(carboxymethyl)-L-lysine trilithium was synthesized according to the literature procedure [17]. The HEMA hydrogels and NTA-containing HEMA hydrogels were synthesized by free-radical photopolymerization with 365 nm UV exposure for typically 5 min. DMPAP was used as the photoinitiator and various concentrations of EGDMA were used as the crosslinking agent. As an example, a HEMA pre-gel solution was prepared by mixing HEMA (30 mL), EGDMA (1 mL), and DMPAP (10 mg). The NTA-monomer solution was made by dissolving NTA monomer (10 mg) in H_2O (350 μL). NTA-containing hydrogel (1 mol.-%) was synthesized by crosslinking an homogeneous mixture of HEMA solution (20 μL) and NTA-monomer solution (20 μL).

Hydrogel fabrication was conducted on a borosilicate glass substrate. These substrates were first soaked in a 1:1:0.5 $H_2O_2/H_2SO_4/H_2O$ solution for 20 min, rinsed with water, then soaked in a 1:1:5 $H_2O_2/NH_3OH/H_2O$ solution for 20 min at 70 °C, rinsed with water and then with isopropyl alcohol and finally dried under nitrogen. The clean substrates were soaked in 10 % v/v of methacryloxypropyl trimethoxysilane in toluene for 1 h. The substrates were then washed in dichloromethane and dried under nitrogen. The substrate can also be treated by hydrophobic trichloro(1*H*,1*H*,2*H*,2*H*-perfluorooctyl) silane for easy lift-off when hydrogel binding to the surface is not desired.

Protein-Binding Studies: A series of control experiments were designed to confirm that protein attachment to the NTA-containing hydrogel took place through specific interaction between Ni-NTA and the histidine residue of the protein. Hydrogels with and without NTA moieties were synthesized in a 96-well polystyrene plate by photopolymerization of 10 μL pre-gel mixtures. Fluorescently labeled ubiquitin was used as the indicator for this binding step. The fluorescence signal was acquired using a SPECTRAFluor plate reader. After nickel sulfate treatment and several washing cycles, results from NTA-containing hy-

ADVANCED FUNCTIONAL MATERIALS

drogel and non-NTA hydrogel were compared. Readings for wells without any hydrogels were also collected as a reference point for plate background. Fluorescently labeled ubiquitin solutions of different dilution (1:100, 1:50, 1:10, 1:5, and 1:2 from 0.8 mg mL^{-1}) were used in this experiment. An experiment that incorporated EDTA in the incubation buffer was also included to demonstrate the need for a stable Ni-NTA complex for efficient protein binding. Hydrogel samples with different mole percentages (0 mol.-%, 0.5 mol.-%, 1.0 mol.-%, and 1.5 mol.-%) of NTA incorporation were prepared to control the amount of protein bound to the surface. Confocal fluorescence microscopy was used to acquire the surface and vertical cross-section images of the hydrogel films.

The activity of surface-bound protein was demonstrated by the microtubule gliding assay. An approximately 20 μm thick by 1 mm wide hydrogel substrate was polymerized on a glass microscope slide. Typically, both a 0 % Ni-NTA and 1 % Ni-NTA gel were polymerized on the same slide with a spacing of roughly 5 mm. The sample chamber was then created between the hydrogel-coated glass microscope slide and a No. 1 cover glass (Corning, Corning, NY) by separating the elements with approximately 100 μm thick double sided Scotch tape (3M, St. Paul, MN). The motility assay was prepared by first pre-incubating the gels with the motility buffer (80 mM piperazine-1,4-bis(2-ethanesulfonic acid), PIPES, 4 mM $MgCl_2$, 20 μM Taxol (paclitexol), 1 mM dithiothreitol, DTT, 1 mM ATP). 1 sample volume of kinesin (recombinant from pPK113) diluted in motility buffer to between 0.5 and 5 μg mL^{-1} was then incubated for several minutes in the sample chamber. The gels were then washed with various amounts of motility buffer (1–10 sample volumes) in an attempt to remove non-specifically bound kinesin. Roughly 10 μm long rhodamine-labeled microtubules (Cytoskeleton TL331M) diluted in motility buffer were then incubated in the sample chamber. The chamber was washed with 1–10 sample volumes of motility buffer to remove unbound microtubules. An oxygen scavenger system (0.1 mg mL^{-1} catalase, 0.03 mg mL^{-1} glucose oxidase, 10 mM glucose, 0.3 % 2-mercaptoethanol) was added in the final wash to reduce fluorescent bleaching.

Received: March 21, 2004
Final version: December 6, 2004

[1] J. T. Finer, R. M. Simmons, J. A. Spudich, *Nature* **1994**, *368*, 112.
[2] K. Svoboda, S. M. Block, *Cell* **1994**, 77, 773.
[3] D. L. Coy, M. Wagenbach, J. Howard *J. Biol. Chem.* **1999**, *274*, 3667.
[4] M. D. Wang, M. J. Schnitzer, H. Yin, R. Landick, J. Gelles, S. M. Block, *Science* **1998**, *282*, 902.
[5] B. Albert, A. Johnson, J. Lewis, M. Raff, K. Roberts, P. Walter, *Molecular Biology of the Cell*, 3rd ed., Garland, New York **1994**.
[6] L. Limberis, R. J. Steward, *Nanotechnology* **2000**, *11*, 47.
[7] H. Suzuki, A. Yamada, K. Oiwa, H. Nakayama, S. Mashiko, *Biophys. J.* **1997**, *72*, 1997.
[8] D. V. Nicolau, H. Suzuki, S. Mashiko, T. Taguchi, S. Yoshikawa, *Biophys. J.* **1999**, *77*, 1126.
[9] J. R. Dennis, J. Howard, V. Vogel, *Nanotechnology* **1999**, *10*, 232.
[10] H. Henry, C. John, Q. Dong, J. Howard, V. Vogel, *Nano Lett.* **2001**, *1*, 235.
[11] Y. Hiratsuka, T. Tada, K. Oiwa, T. Kanayama, T. Uyeda, *Biophys. J.* **2001**, *81*, 1555.
[12] K. Y. Lee, D. J. Mooney, *Chem. Rev.* **2001**, *101*, 1869.
[13] S. V. Vinogradov, T. K. Bronich, A. V. Kabanov, *Adv. Drug Delivery Rev.* **2002**, *54*, 135.
[14] M. D. Lang, R. P. Wong, C. C. Chu, *J. Polym. Sci., Part A: Polym. Chem.* **2002**, *40*, 1127.
[15] M. Slivka, C. C. Chu, Y. L. Zhang, *J. Mater. Sci.: Mater. Med.* **2001**, *12*, 241.
[16] Y. L. Zhang, C. C. Chu, *J. Biomed. Mater. Res.* **2002**, *59*, 318.
[17] B. R. Hart, K. J. Shea, *J. Am. Chem. Soc.* **2001**, *123*, 2072.
[18] C. Wang, R. J. Stewart, J. Kopecek, *Nature* **1999**, *397*, 417.
[19] *QIAexpress Detection and Assay Handbook*, QIAGEN Inc., Valencia, CA **1999**.
[20] C. Ho, L. Limberis, K. D. Caldwell, R. J. Stewart, *Langmuir* **1998**, *14*, 3889.
[21] T. Yu, C. K. Ober, *Biomacromolecules* **2003**, *4*, 1126.
[22] F. Chiellini, D. Schmaljohann, T. Yu, R. Solaro, E. Chiellini, C. K. Ober, *Macromol. Rapid Commun.* **2001**, *22*, 1284.
[23] J. F. Hainfeld, W. Liu, C. M. R. Halsey, R. Freimuth, R. D. Powell, *J. Struct. Biol.* **1999**, *127*, 185.
[24] Y. Hiratsuka, T. Tada, K. Oiwa, T. Kanayama, T. Q. Uyeda, *Biophys. J.* **2001**, *81*, 1555.
[25] J. Rietdorf, A. Ploubidou, I. Reckmann, A. Holmstrom, F. Frischknecht, M. Zettl, T. Zimmermann, M. Way, *Nat. Cell Biol*. **2001**, *3*, 992.

